

GLOBAL SURFACE SOLAR ENERGY ANOMALIES INCLUDING EL NINO AND LA NINA YEARS

C. H. Whitlock, D. E. Brown, W. S. Chandler,
and R. C. DiPasquale
Science Applications International Corporation
One Enterprise Parkway, Suite 300
Hampton, VA 23666-5845
(757) 827-4882
c.h.whitlock@larc.nasa.gov

Shashi K. Gupta and Anne C. Wilber
Analytical Services & Materials, Inc.
One Enterprise Parkway, Suite 300
Hampton, VA 23666-5845
(757) 827-4621
s.k.gupta@larc.nasa.gov

Nancy A. Ritchey
Computer Sciences Corporation
3217A North Armistead Ave
Hampton, VA 23666-1379
(757) 864-9813
n.a.ritche@larc.nasa.gov

David P. Kratz, and Paul W. Stackhouse
NASA Langley Research Center
Hampton, VA 23681-0001
(757) 864-5669
d.p.kratz@larc.nasa.gov

ABSTRACT

Atypical weather conditions are known to occur for extended periods of time that either may or may not coincide with El Nino and La Nina events in the Pacific Ocean. Anomalies that increase clouds influence the reliability of both renewable energy and building environmental-control systems. Backup equipment on non-grid solar power systems may run out of capacity for such items as communications electronics, flood-warning stream gages, refrigerators, and small village power systems in remote regions. This paper provides 1x1-degree resolution global maps that identify those regions which experienced large abnormal solar energy during a 10-year period. A source is identified where specific values for maximum year-to-year variability can be obtained in regions where ground-site measurements do not exist.

INTRODUCTION

This paper synthesizes past events in an attempt to define the general magnitude, duration, and location of large surface solar anomalies over the globe. Surface solar energy values are mostly a function of solar zenith angle, cloud conditions, column atmospheric water vapor, aerosols, and surface albedo. For this study, solar and meteorological parameters for the 10-yr period July 1983 through June 1993 are used. These data were generated as part of the Release 3 Surface meteorology and Solar Energy (SSE) activity under the NASA Earth Science Enterprise (ESE) effort. Release 3 SSE (<http://eosweb.larc.nasa.gov/sse>) uses upgraded input data and methods relative to previous releases. Cloud conditions are based on recent NASA Version-D

International Satellite Cloud Climatology Project (ISCCP) global satellite radiation and cloud data (<http://isccp.giss.nasa.gov>). Meteorological inputs are from Version-1 Goddard Earth Observing System (GEOS) reanalysis data that uses both weather station and satellite information (<http://dao.gsfc.nasa.gov>). Aerosol transmission for different regions and seasons are for an "average" year based on historic solar energy data from over 1000 ground sites courtesy of Natural Resources Canada (NRCan) at <http://retscreen.gc.ca>. These data are input to a new Langley Parameterized Shortwave Algorithm (LPSA) that calculates surface albedo and surface solar energy. That algorithm is an upgraded version of the "Staylor" algorithm described in Whitlock et al. (1995), Darnell et al. (1996), and Gupta et al. (1999). Calculations are performed for a 280 x 280 km equal-area grid system over the globe based on 3-hourly input data. A bi-linear interpolation process is used to estimate data output values on a 1 x 1 degree grid system over the globe.

Maximum anomalies are examined relative to El Nino and La Nina events in the tropical Pacific Ocean. Maximum year-to-year anomalies over the globe are provided for a 10-year period. The data may assist in the design of systems with increased reliability. It may also allow for better planning for emergency assistance during some atypical events.

COMPARISON OF SATELLITE INSOLATION WITH GROUND MEASUREMENTS

Historical ground measurements were obtained from Natural Resources Canada's CANMET Energy

Diversification Research Laboratory (CEDRL) and the National Renewable Energy Laboratory (NREL). The 30-year average RETScreen™ database from CEDRL contains temperature, wind, humidity, and solar energy data from more than 1000 sites (<http://retscreen.gc.ca>). NREL distributes the World Radiation Data Center (WRDC) monthly surface solar energy measurements for 1195+ sites from 1964 through 1993 (<http://wrdc-mgo.nrel.gov>). All ground stations were not operating for every year in either data set. Therefore, various years of data contained different combinations of ground site locations. When more than one ground measurement station was located in a grid cell, the ground measurements were averaged for comparison to the SSE data.

It is generally believed that quality measured ground data are more accurate than satellite-derived values. Unfortunately, measurement uncertainties are not precisely known for either ground site data set. For this reason, SSE differences from ground measurements are considered as estimates of uncertainty.

Following usual industry standards, estimated uncertainty is the Root-Mean-Square (RMS) difference when large sample sizes exist and statistical correlation has been performed. Bias is included in the RMS values. Estimated uncertainties over the 10-year data period are given in Table 1 from Whitlock et al. (2000). Slight RMS increases during El Nino and La Nina years may be caused by localized abnormal aerosols (i.e., smoke and pollution) or water vapor as a result of droughts and wind changes that might not have been detected by satellite or reanalysis data. Average bias differences for the WRDC data set range from -2.0% to +3.3% depending on the year. Thirty-year average RETScreen data bias differences range from +1.0% to +2.5% depending on the near-average year. Bias and RMS results suggest that the Release 3 satellite-based values follow similar geographical and time-history trends as ground-site measurements. Release 3 SSE results may be useful to energy system designers in remote regions without quality ground site measurements.

EL NINO/LA NINA EVENTS

Under normal conditions, easterly trade winds near the equator in the tropical Pacific cause a warm water pool to form in the west Pacific. This creates sea surface temperatures about 8°C higher in Indonesia than those off the coast of Ecuador.

When El Ninos exist, weaker than normal trade winds occur in the central and western Pacific. The warm water pool drifts eastward warming the atmosphere over the eastern Pacific causing changes in atmospheric circulation that affect regions in other parts of the globe. In the December through January period, warmer-than-normal temperatures are reported to occur in the northeast U.S., eastern Canada, western Canada, north central U.S., Japan, eastern and southern China, Burma, India, southern

Australia, and southeast Brazil. Droughts occur in Indonesia. Unusually wet conditions may occur in Peru and Ecuador. June through August anomalies typically cause droughts in India, Indonesia, and eastern Australia. Wetter-than-normal weather occurs in the northwestern U.S. and northern Chile (<http://iri.ldeo.columbia.edu/climate/dictionary/enso/impacts.html>, <http://www.pmel.noaa.gov/toga-tao/el-nino-story.html>, <http://www.pmel.noaa.gov/toga-tao/la-nina-story.html>, and <http://iri.ldeo.columbia.edu/climate/dictionary/enso/ensoevent.html>).

Under La Nina conditions, stronger than normal trade winds push the warm water pool further west which allows colder water from South America to flow further west along the Equator. Changing both the warm and cold water locations again changes atmospheric heating locations and circulation patterns in many regions of the globe. La Nina impacts are believed to be opposite those from El Nino on a global scale.

Scientists have discovered a correlation of the difference in surface atmospheric pressure between Darwin, Australia and Tahiti and the seesawing of the warm water pool between the eastern and western sides of the tropical Pacific Ocean. The Southern Oscillation Index (SOI) is the Tahiti minus Darwin pressure difference standardized by the 1951 to 1980 mean annual standard deviation. It is usually correlated with surface water temperature measurements on the Equator at 110 degrees West. Negative values of SOI usually indicate warmer-than-normal El Nino water conditions, and positive values suggest cooler-than-normal La Nina water.

Owners and operators of renewable energy systems can now obtain near-real-time status of both the 110 degree West water temperature and the SOI (http://www.pmel.noaa.gov/toga-tao/gif/daily/soi_110w_80.gif). Forecasts of oncoming events are also available (http://www.pmel.noaa.gov/toga-tao/el_nino/forecasts.html). Little information is available on changes in cloud cover and solar energy reaching the Earth's surface, however.

SURFACE SOLAR ENERGY DURING NEAR-AVERAGE AND EL NINO/LA NINA YEARS

El Nino and La Nina events vary in strength, timing, and duration. The magnitudes of SOI and water temperature deviation are shown in Fig. 1, courtesy of the http://www.pmel.noaa.gov/toga-tao/gif/daily/soi_110w_80.gif web site. If either or both indicators differ from zero by more than 0.5 (or 0.5°C), an El Nino or La Nina may be occurring. The time period of the SSE data used in this study are shown by the initial and final vertical dashed lines. Other lines show the beginning of each year. Note that the unusual high-strength El Ninos

in 1982-1983 and 1997-1998 are not included in the present SSE data set. Appropriate satellite data are not yet available for these two time periods.

Figure 1 the graph's solid lines represent 5-month running means that do not always indicate the same thing is happening. There appear to be time lags with either parameter leading the other by some months at various time periods. Near-average years based on the SOI definition may contain either an El Nino or a La Nina based on temperature variation. This inconsistency appears to be carried over into surface solar energy values. Two remote regions where El Ninos and La Ninas are known to have a strong influence are examined below:

1. In the above El Nino scenarios, winter droughts occur in Indonesia and northern Australia. This study finds that surface solar energy does not always follow the expected pattern of fewer clouds. Indonesia had both 20% more solar energy (January, 1992) and 20% less solar energy (January, 1987) for the same values of SOI (-2) and 110-deg West temperature deviation (+2°C).

2. The above El Nino scenarios suggest large amounts of winter rain in western South America, suggesting more clouds. The same $\pm 20\%$ opposite solar energy variation occurs in western South America during the above two January El Nino dates.

Reviews of individual monthly solar insolation maps for the globe show similar inconsistency in other regions for the mid-strength El Ninos and La Ninas contained in this particular 10-yr data period. Additional work is required to develop more reliable indicators of surface solar energy variations related to El Nino and La Nina events. Those studies are suggested when appropriate satellite data for the high-strength El Ninos in 1982-1983 and 1997-1998 become available. It appears safer for system designers and plant operators to continue decisions based on maximum anomalies at this time.

10-YEAR MAXIMUM SOLAR ENERGY ANOMALIES

Figures 2(a) through 2(f) show maximum surface solar energy deficits and excesses relative to 10-year average values over the globe. Deficits are given as the percent of solar energy that was not available relative to the expected average value for the month. Excess is the percent above the monthly average expected. Maps for every other month are shown for reasons of brevity. The maps show regions of unusual stability ($\pm 5\%$ white areas) in spite of weather events such as El Ninos and La Ninas. Most of the globe appears to have year-to-year variability within $\pm 15\%$. Many regions have higher variability for only a few months that may or may not be critical to a particular solar-energy system. There are a few land regions with very large variability ($>45\%$). These are the Arctic coasts,

central China, portions of Europe, and small regions in Canada.

System designers may use Fig. 2 for quick assessment of the general magnitude of maximum year-to-year variability in various regions of the globe. Values for a specific location may be obtained as described below.

THE NASA RELEASE 3 SSE WEB SITE

More precise information for specific locations can be obtained from the NASA Release 3 SSE web site (<http://eosweb.larc.nasa.gov/sse>). Meteorology, wind, surface albedo, and surface solar energy parameters can be obtained for each 1-degree cell over the globe subject to uncertainties described in both the Methodology and Accuracy sections of the web site. Monthly average, maximum, minimum, 1987 El Nino, and 1988 La Nina surface solar energy values are given for each cell. These may be useful for preliminary selection and sizing of systems. Within-month information is also provided that is useful for the design of both backup systems and storage of surplus product. Maximum consecutive-day deficits and surpluses are available in several forms including the Equivalent No-Sun (or Black) Day design parameter. These values are obtained based on 3-hourly NASA SSE information over the entire 10-yr period.

CONCLUDING REMARKS

Atypical events are known to occur for extended periods of time. Anomalies that increase clouds, aerosols, or water vapor may influence the reliability of both renewable energy and building environmental-control systems. This paper provides global maps that identify those regions that experienced significant variation in the surface solar energy resource over a 10-yr period. The maps are useful for quickly estimating the order-of-magnitude of maximum variability. A source for more detailed information at specific locations has been provided.

REFERENCES

- Darnell, W. L., Staylor, W. F., Ritchey, N. A., Gupta, S. K., and Wilber, A. C., 1996, "Surface Radiation Budget: A Long-term Global Dataset of Shortwave and Longwave Fluxes." *American Geophysical Union*, <http://www.agu.org/eos_elec/95206e.html>.
- Gupta, S. K., Ritchey, N. A., Wilber, A. C., Whitlock, C. H., Gibson, G. G., and Stackhouse, P. W., Jr., 1999, "A Climatology of Surface Radiation Budget Derived From Satellite Data." *J. Climate*, Vol. 12, 2691-2710.
- Whitlock, C. H., Charlock, T. P., Staylor, W. F., Pinker, R. T., Laszlo, I., Ohmura, A., Gilgen, H., Konzelmann,

T., DiPasquale, R. C., Moats, C. D., LeCroy, S. R., and Ritchey, N. A., 1995, "First Global WCRP Surface Radiation Budget Data Set." *Bulletin American Meteorology Society*, Vol. 76, No. 6, June, pp. 905-922.

Whitlock, C. H., Brown, D. E., Chandler, W. S., DiPasquale, R. C., Meloche, N., Leng, G. J., Gupta, S. K., Wilber, A. C., Ritchey, N. A., Carlson, A. B., Kratz, D. P., and Stackhouse, P. W., 2000, "Release 3 NASA Surface Meteorology and Solar Energy Data Set for Renewable Energy Use." Proceedings, Rise and Shine 2000, the 26th Annual Conference of the Solar Energy Society of Canada Inc. and Solar Nova Scotia, October 21-24, Halifax, Canada.

Table 1. Estimates of Insolation RMS Uncertainty Including Bias.

Time Period	Global Interior Regions WRDC Site Data	Global Coastal Regions WRDC Site Data	Global All Regions RETScreen Site Data
Near-Average Years			
1983-2nd Half	11.7%	12.9%	
1984	13.8%	13.1%	13.9%
1985	13.5%	12.5%	13.1%
1986	13.1%	13.7%	12.6%
1990	15.5%	15.4%	13.4%
El Nino Years			
1987	14.5%	14.6%	
1991	17.0%	15.3%	
1992	15.4%	13.7%	
1993-1st Half	14.9%	15.4%	
La Nina Years			
1988	14.8%	13.8%	
1989	14.9%	13.9%	

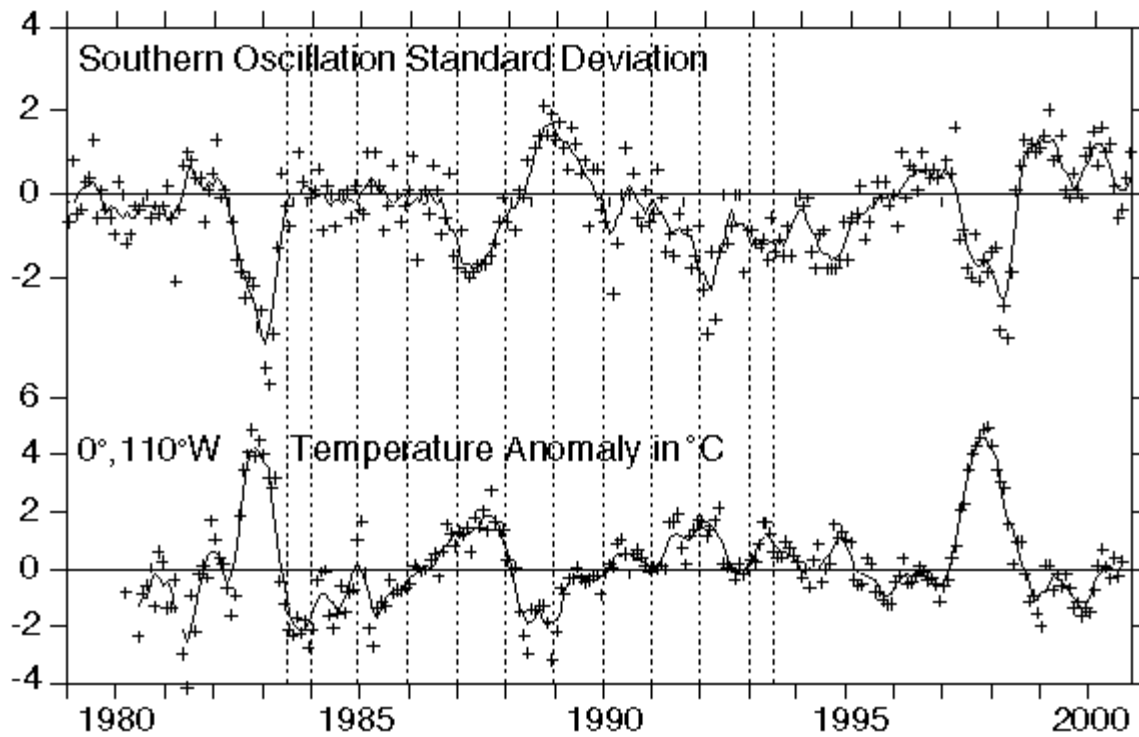


Fig: 1 Time histories of Southern Oscillation Index and equatorial water temperature deviation at 110 deg west.

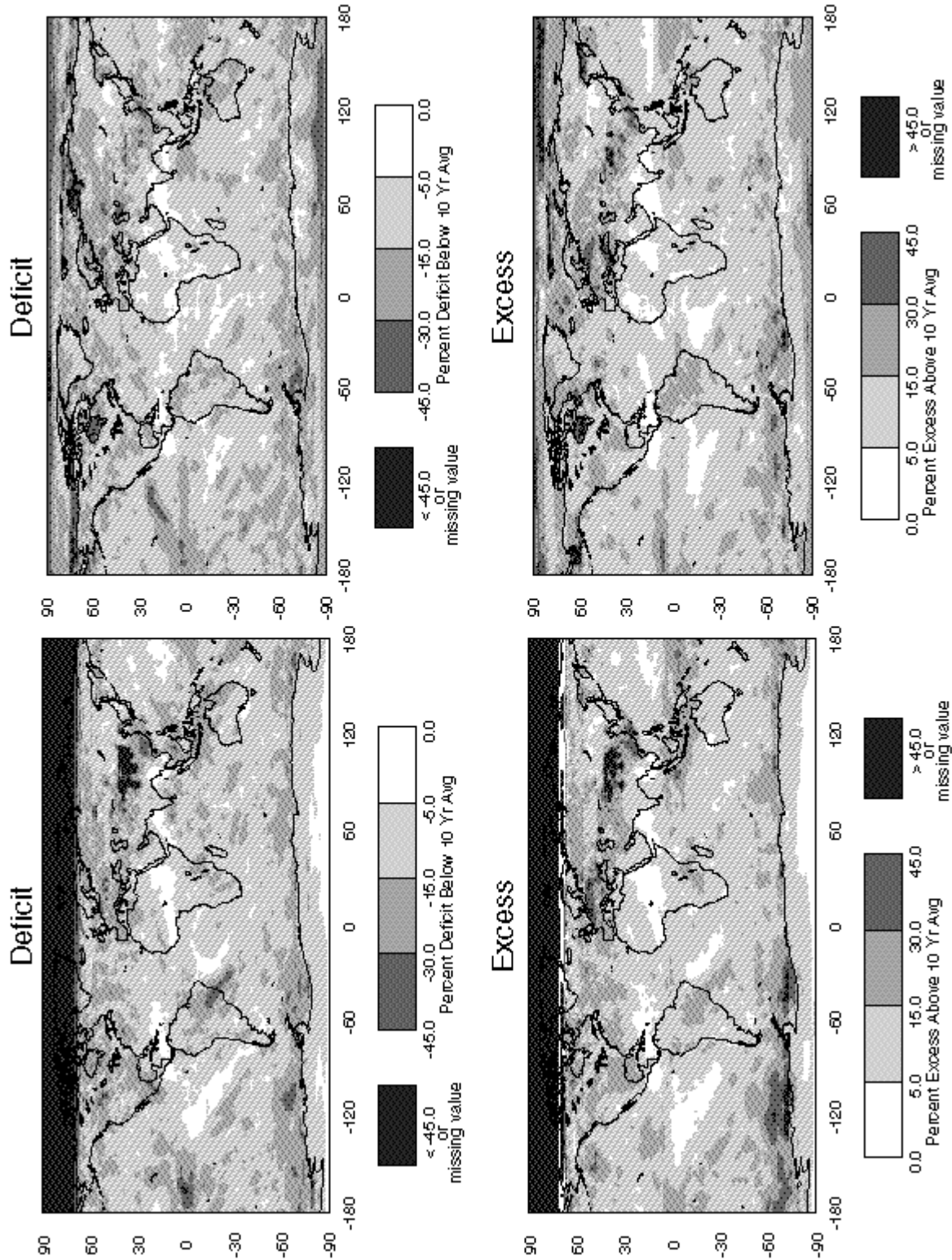


Fig 2(b): March Deficit and Excess Insolation Relative to 10-yr Average.

Fig 2(a): January Deficit and Excess Insolation Relative to 10-yr Average.

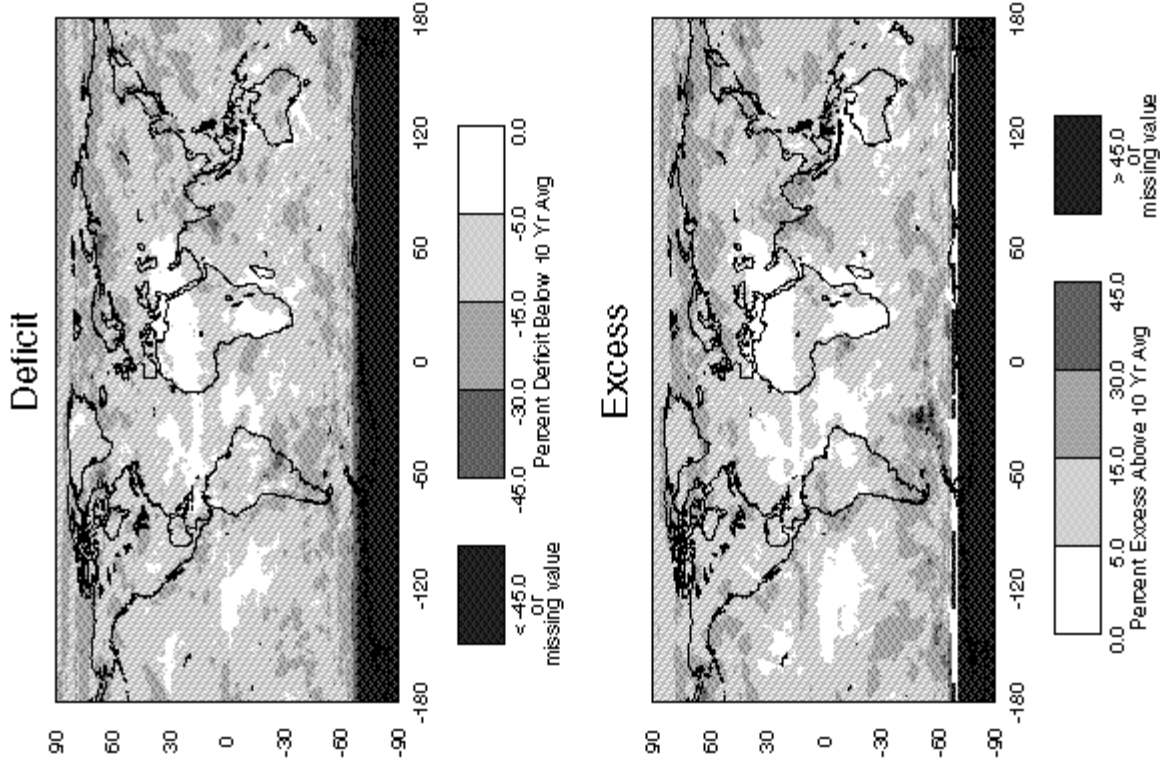


Fig 2(d): July Deficit and Excess Insolation Relative to 10-yr Average.

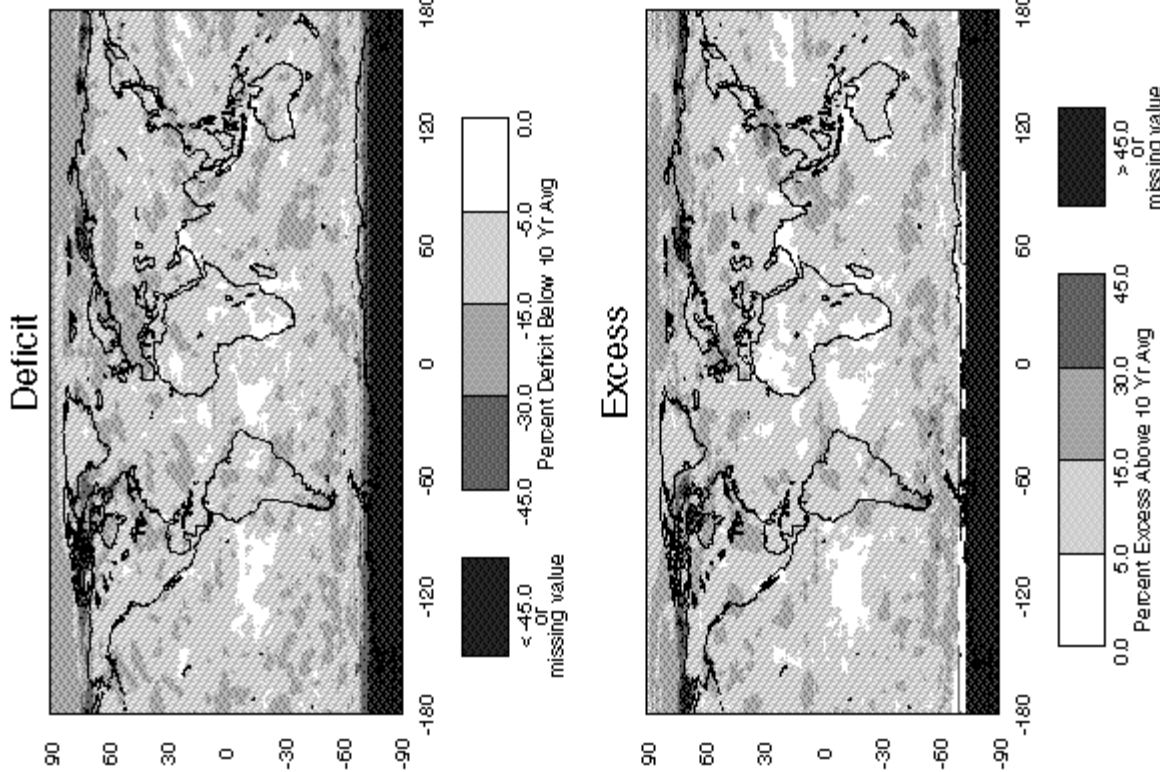


Fig 2(c): May Deficit and Excess Insolation Relative to 10-yr Average.

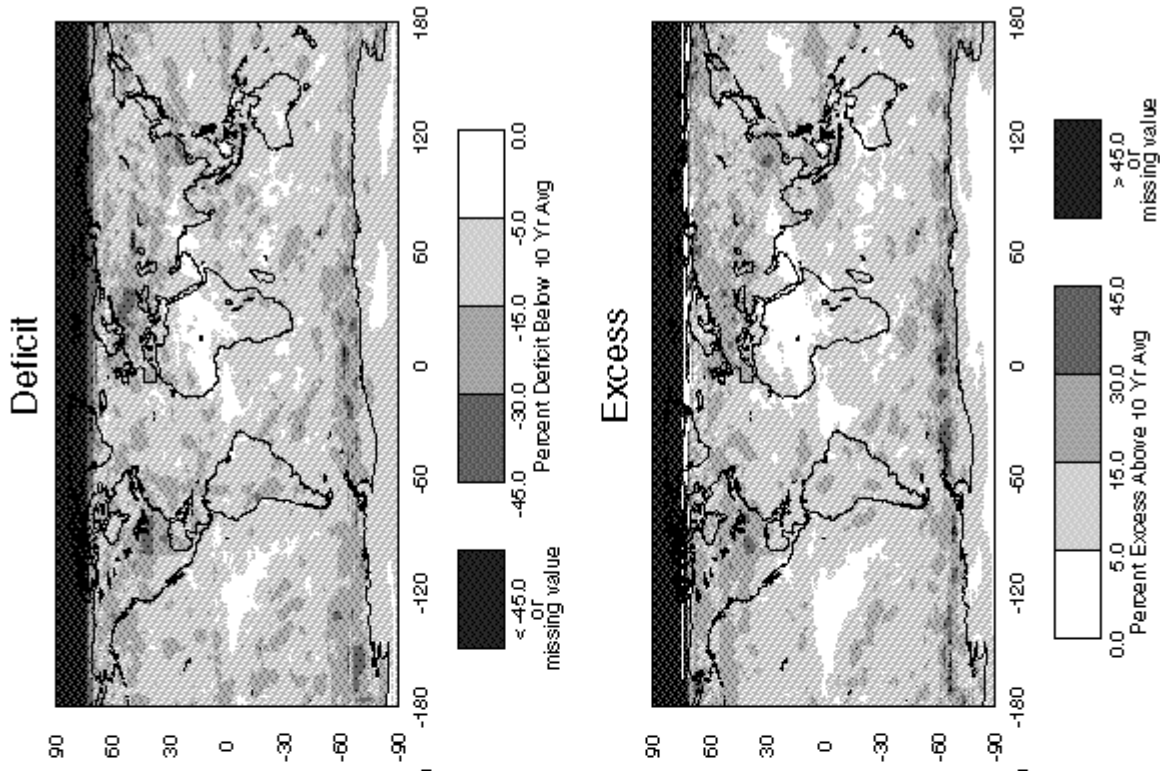


Fig 2(f): November Deficit and Excess Insolation Relative to 10-yr Average.

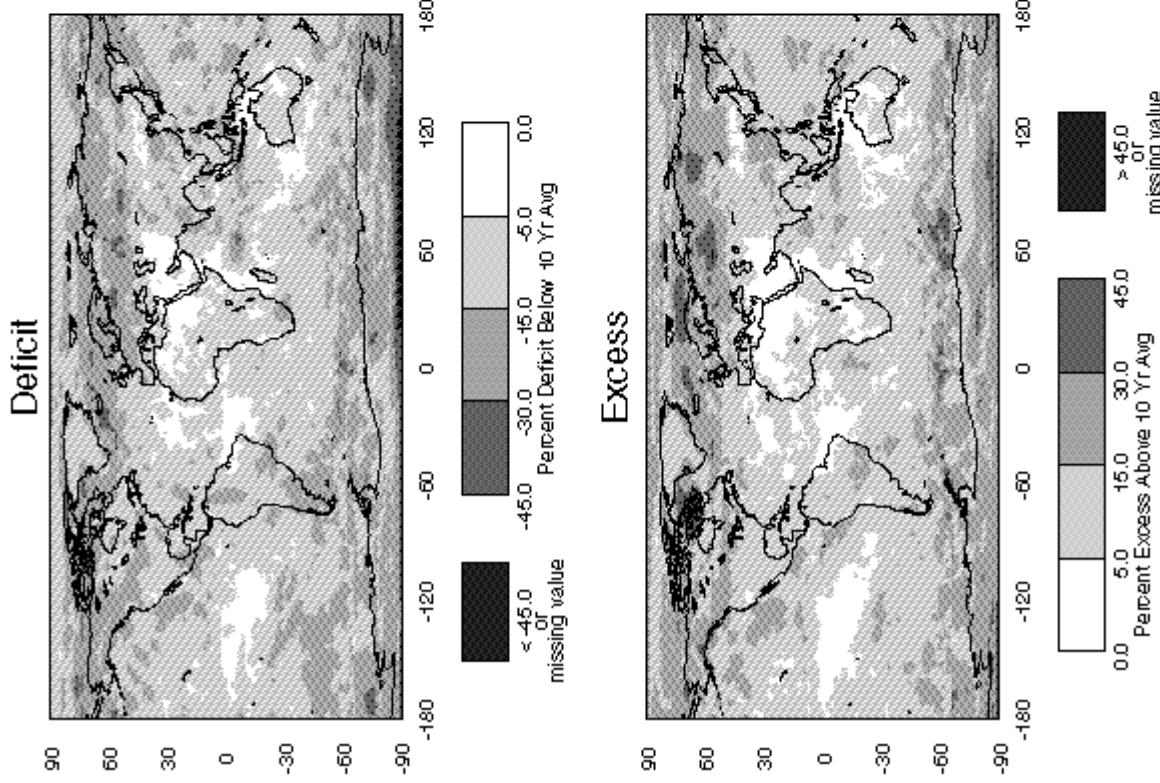


Fig 2(e): September Deficit and Excess Insolation Relative to 10-yr Average.